Appl Phys B (2012) 106:399–404
DOI 10.1007/s00340-011-4706-x

Applied Physics B
Lasers and Optics

Spectral dependence of transient reflectance in a ZnO epitaxial film at room temperature

P.-C. Ou · J.-H. Lin · W.-F. Hsieh

Received: 24 April 2011 / Revised version: 28 June 2011 / Published online: 9 September 2011
© Springer-Verlag 2011

Abstract We demonstrated the spectral dependence of time-resolved reflectance in a ZnO epitaxial film at room temperature. The ultrafast thermalization time increases as increasing the excitation photon energy accompanied with the hot phonon effect. The obtained recovery time of renormalized bandgap, associated with the nonradiative decay or the free exciton formation, is independent of photon energy. Based on a theoretical model to calculate the carrier-induced change of refractive index in ZnO, the spectral dependent transient reflectance can be successfully analyzed as a result of combined effects of band-filling (BF) and bandgap renormalization (BGR). The measured transient reflectance decreases with decreasing the photon energy for excitation above the bandgap states revealing the significance of competition of the BF and BGR effects.

1 Introduction

Zinc oxide (ZnO), a direct semiconductor with wide bandgap energy of 3.37 eV and large exciton binding energy of 60 meV, has attracted much attention as a promising candidate for room temperature (RT) photonic devices in the blue to UV spectral region [1, 2]. During the past few years, advances in epitaxial growth with either plasma-assisted molecular-beam epitaxy (P-MBE) or pulsed laser deposition (PLD) on sapphire substrates can produce high quality ZnO epitaxial layers [3, 4]. Optically pumped stimulated emission and lasing from exciton–exciton scattering and the electron–hole plasma (EHP) have been demonstrated in ZnO epitaxial films at RT or even at the elevated temperature [3–5]. Our previous studies measured the steady-state nonlinear absorption near the IR region and UV region to realize the detail optical information in ZnO by using the Z-scan method [6, 7].

Recently, there were some reports about the carrier dynamics in ZnO [8–15], and most studies focused on the lasing dynamics and excitonic recombination by using the time-resolved PL. Under high excitation, Takeda et al. [8, 9] studied the transient EHP emission in ZnO by using the optical Kerr gate method. In their reports, the formation of EHP emerges with a delay time of 4–6 ps under band-to-band excitation; while it happens instantaneously under exciton resonance excitation. In contrast to transient PL measurement, the optical pump-probe technique is capable of probing ground state bleaching as well as excited-state absorption. Bauer et al. performed the femtosecond transient absorption with the probe wavelength dependence in the red-IR region and observed the ultrafast decay time around 1 ps due to the trapping of nonequilibrium carriers by using the non-degenerate pump-probe technique in ZnO [12]. Besides, Acharya et al. have shown the transient absorption of discrete exciton bleaching and investigated the influence of $BaTiO_3$ layer on the charge carrier dynamics of ZnO by measuring the pump-probe spectroscopy in ZnO and $ZnO/BaTiO_3$ thin films [13]. The pumping intensity depen-

P.-C. Ou · W.-F. Hsieh (✉)
Department of Photonics and Institute of Electro-optical Engineering, National Chiao Tung University, Hsinchu 300, Taiwan
e-mail: wfhsieh@mail.nctu.edu.tw
Fax: +886-3-5716631

J.-H. Lin
Department of Electro-optical Engineering, National Taipei University of Technology, Taipei 106, Taiwan
e-mail: jhlin@ntut.edu.tw

W.-F. Hsieh
Institute of Electro-optical Science & Engineering and Advanced Optoelectronics Technology Center, National Cheng Kung University, Tainan 701, Taiwan

dent dynamics reveals transition of excitonic relaxation from exciton–phonon scattering into exciton–exciton scattering, when we demonstrated the transient differential transmission in ZnO under exciton resonant excitation [14]. Our previous studies also reported that the surface trapping reduce the probability of carrier–phonon scattering to result in a prolonged thermalization time (∼10 ps) under band-to-band excitation in a thin ZnO sample with thickness less than 100 nm [15]. Furthermore, with increasing carrier concentration in Ga-doped ZnO [16], the doping-induced band-filling (BF) effect causes a blue shift to the absorption spectral edge, while the doping-induced bandgap renormalization (BGR) effect results in a red shift to the near band-edge PL emission.

In order to directly monitor the ultrafast thermalization without taking surface trapping into account and realize the temporal evolution of free carriers convert into free excitons, we performed the carrier dynamics in a thick ZnO sample with excitation energy from well above bandgap states to near exciton resonance by utilizing the pump-probe technique at RT. We demonstrate the spectral dependent time-resolved photo-reflectance and show the significance of competition of BF and BGR effects in this work. It can be observed that the ultrafast thermalization time increases with increasing the photon energy via the assistance of hot phonon emission. The recovery time of renormalized bandgap can be obtained and the measured exciton lifetime is comparable to previous time-resolved PL studies [11]. Moreover, the performance reveals that the interplay between BF and BGR effects determines the magnitude and sign of transient reflectance. Based on a theoretical model [17] to calculate the change of refractive index induced by the BF and BGR effects in ZnO under quasiequilibrium, we successfully interpret the spectral dependence of transient reflectance.

2 Experiment

Our c-axis oriented ZnO epitaxial film with thickness of 1 μm was grown on a c-plane sapphire substrate with high vacuum of 2.1×10^{-8} Torr by pulsed laser deposition with a KrF excimer laser [18]. Hall measurements yielded a background electron concentration of 1.87×10^{17} cm^{-3}. The absorption spectrum was measured using spectral photometer (Jason V-670) with resolution of 0.5 nm at RT. Due to large absorption coefficient of 2×10^5 cm^{-1} near the band-edge, the transmitted light is too weak to be detected when the sample is thicker than 500 nm; and the reflection type measurement is required. The time-resolved optical pump-probe measurements were also performed at RT using a frequency doubled mode-locked Ti:sapphire laser with 82 MHz repetition rate (Tsunami, Spectral Physics Inc.) equipped

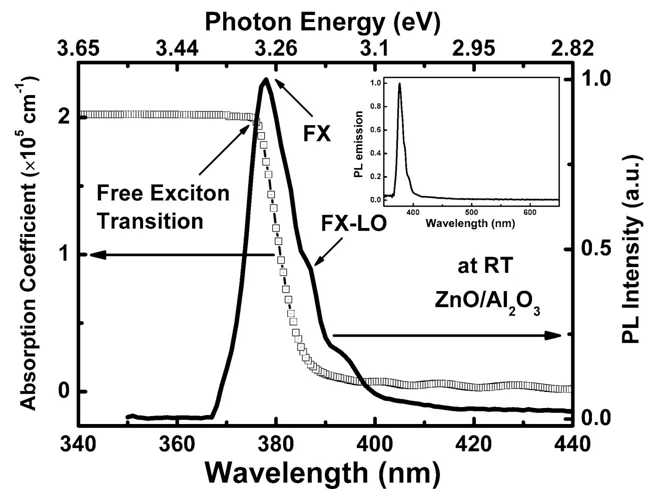

Fig. 1 Room temperature absorption spectrum (*hollow squares*) and time-integrated PL spectra (*solid line*) of a ZnO epitaxial film grown on a sapphire substrate. *Inset*: Time-integrated PL with a longer wavelength scale

with a frequency doubler (Model 3980), providing ultraviolet (UV) excitation wavelength with pulse width around 150 fs. The UV beam was divided by a beam splitter into a pump beam and a probe beam with intensity ratio larger than 20:1. The probe beam passed through a motorized translation stage in order to control the time delay relative to the pump one. The pump and the probe beams were focused and overlapped onto the sample surface by a focal lens with focal length of 5 cm. These two beams made a small angle of 10 degrees and the beam diameter of pump beam is slightly larger than that of probe beam. For the purpose of reducing the artifact, the polarizations of pump and probe beams were orthogonal to each other by using a half-wave plate. In addition, we put an iris and a polarizer with its polarization parallel to the probe beam before the detector to filter out the scattered light from the pump beam. In order to increase the signal-to-noise ratio, the pump beam was modulated at 1 kHz by a mechanical chopper, and the reflected probe beam was detected by a photo-diode and measured as a function of time delay by a lock-in amplifier. The time-resolved setup is similar to the previous experimental arrangements [19]. In addition, the time-integrated photoluminescence (TIPL) excited by this pulsed laser was measured using a single grating monochromator (iHR320) at RT.

3 Results and discussion

3.1 Absorption and TIPL spectra at RT

Figure 1 showed the measured absorption spectrum and time-integrated (TI) PL spectra of the c-plane ZnO epitaxial film on sapphire substrate at room temperature (RT). It reveals an absorption spectral edge at 376.5 nm or 3.294 eV

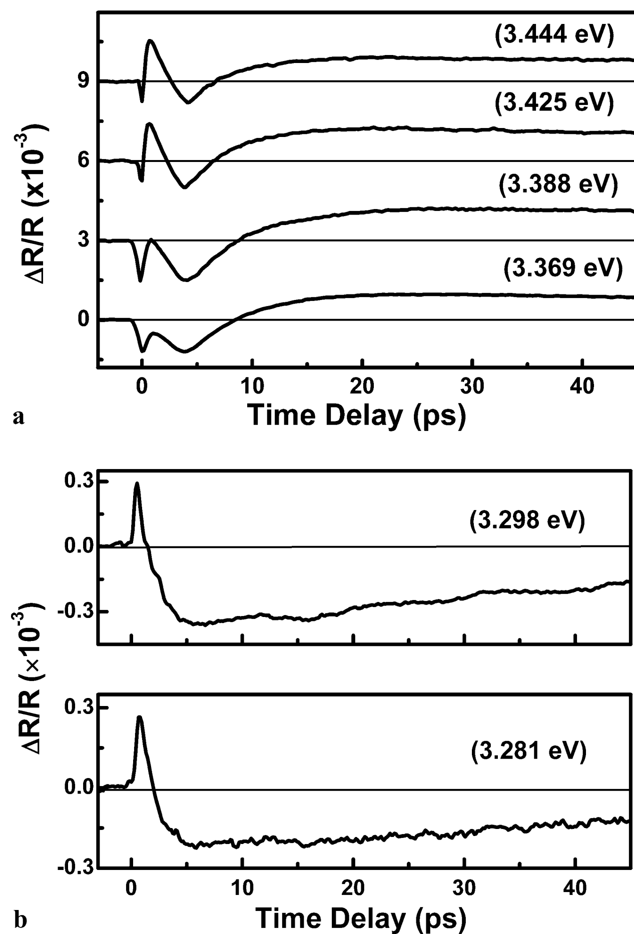

Fig. 2 Measurement of transient normalized differential reflectance as a function of time delay. (**a**) For excitation photon energy at 3.444, 3.425, 3.388, and 3.369 eV. Traces are vertically displaced for clarity. (**b**) For excitation photon energy at 3.298 and 3.281 eV

corresponding to the free exciton transition. Considering the exciton binding energy of 60 meV, the bandgap energy (E_g) is around 3.354 eV or 369.7 nm. The linear absorption coefficient near the bandedge is around 2×10^5 cm^{-1}. Under inter-band excitation at RT, the TIPL spectra reveal a peak of 378 nm or 3.280 eV corresponding to excitonic spontaneous emission with FWHM of 98 meV. Due to large exciton and LO-phonon coupling, the LO-phonon replica can be observed on the low energy shoulder. The inset shows the TIPL spectra with a longer wavelength scale indicating a high contrast ratio of UV to defect emission. Throughout this pump-probe experiment, the pumping fluence on the sample surface is set around 10 μJ/cm^2.

3.2 Spectral dependent ultrafast dynamics

The transient normalized differential reflectance ($\Delta R/R$) as a function of time delay for excitation photon energy above the bandgap at 3.444, 3.425, 3.388, and 3.369 eV were shown in Fig. 2(a). First, around zero time delay we found a negative dip resulting from two-photon absorption (TPA) of simultaneously absorbing one pump and one probe photon. After the TPA, a peak appears due to initially excited free carriers by the pump pulse and then quickly decreases to negative differential reflectance. The negative transient differential reflectance slowly reduces to the original $\Delta R = 0$ level and then transits to a positive one. Finally, there is a relatively slow decay at long time delay. It can be seen that these four traces are similar except that the peak amplitude decreases with decreasing the photon energy. When we performed the carrier dynamics near the free exciton transition, the measured transient $\Delta R/R$ for the photon energy at 3.298 and 3.281 eV in Fig. 2(b) showed completely different dynamics from those of the above bandgap cases. An instantaneous rising by the pump pulse can be observed at the beginning with no apparent TPA effect. The positive transient differential reflectance quickly decreases and then transits to a negative one followed by a slow recovery.

To analyze the measured temporal traces in Fig. 2(a), a decomposition fitting procedure is used to extract the phenomenological responses and their time constants after zero time delay by $a_1 \exp(-t/\tau_1) - a_2 \exp(-t/\tau_2) + a_3 \exp(-t/\tau_3)$. The fitting results for excitation photon energy at 3.444 eV is shown in Fig. 3(a) and similar process can be done for the rests. We show the fitted time constants of τ_1 and τ_2 as a function of excitation photon energy in Fig. 3(b). In general, the generated hot carriers will be scattered away from their initial optically-excited states through either carrier–carrier scattering during coherent regime within a very short time scale less than 200 fs or external thermalization via carrier–phonon scattering to achieve quasiequilibrium with the lattice system. Then the hot carriers release their excess kinetic energy through phonon emission and relax to the bottom of the conduction band. Because the pulse-width of used excitation laser is around 150 fs, we are not supposed to observe the carrier–carrier scattering. Thus, the obtained ultrafast decay time τ_1 around 1.0–1.5 ps is mainly due to the carrier–phonon scattering. This is comparable to previous studies in GaAs [20] and AlGaAs [21], which reported an external thermalization time on the order of 0.9–1.5 ps. As shown in Fig. 3(b), the performed decay time τ_1 slightly decreases with decreasing the photon energy. A strong hot phonon effect is expected in ZnO because of large LO-photon energy around 72 meV. As a consequence, the free carrier thermalization is affected by the assistance of optical-phonon for well above bandedge states; while it is mainly due to the assistance of acoustic-phonon for near band-edge states (excess energy <26 meV).

The time constant τ_2 on the order of 4.6–5.0 ps is comparable to our previous results due to non-radiative decay by measuring the transient differential transmission in a ZnO epilayer with a thickness of 70-nm [15]. It is interesting to compare the measured results with the previous time-resolved PL studies in ZnO thin films and nanostructures.

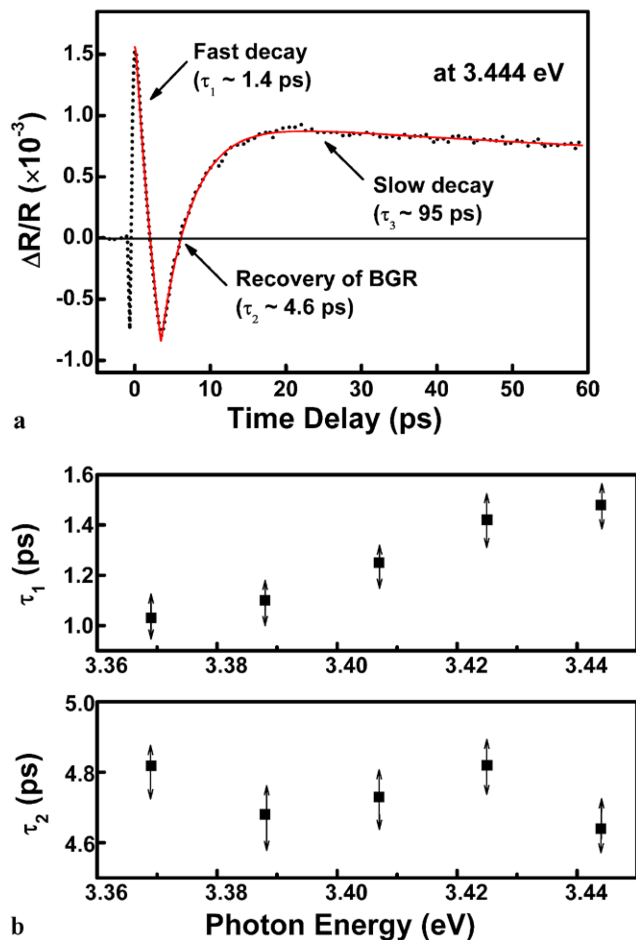

Fig. 3 (**a**) The measurement of time-resolved reflectance (*dotted line*) and the fitting curve (*solid line*) with their corresponding decay time constants for excitation photon energy at 3.444 eV. (**b**) The fitted first and second time constants as a function of photon energy. The arrows indicate the error bar

Previous time-resolved PL reports showed a blue shift of PL emission with a time constant of 2.5 ps due to the recovery of the renormalized bandgap in ZnO thin films by using the optical Kerr gate method [8]. Takeda et al. [9] found that the P-band emission after a time delay of 4.5 ps accompanied with free carriers convert into free excitonic state under band-to-band excitation. Kwok et al. [10] measured the decay times of 7 ps and 10 ps in ZnO rods and shells, respectively, which most likely due to non-radiative decays. The obtained time constant τ_2 is almost independent of photon energy that means the recovery time is concerned with the decay rate of thermalized carriers with Fermi–Dirac distribution near the minimum of renormalized band-edge. Here, we attributed τ_2 to the recovery process of renormalized bandgap accompanied with the decrease of free carriers via nonradiative channel, such as multiphonon emission, trapping by defects, Auger recombination, and forming excitons. The measured third time constant τ_3 on the order of 90–100 ps, independent of the photon energy, is attributed to exciton and/or free carrier recombination. In addition, by using the response function of biexponential decay $a_1 \exp(-t/\tau_f) - a_2 \exp(-t/\tau_s)$ to fit the temporal traces in Fig. 2(b), a fast (τ_f) and a slow (τ_s) decay time constants of 0.8 and 80 ps can be obtained, respectively. Acharya et al. demonstrated the transient absorption measurement to observe the exciton bleaching and obtained the decay time around 1 ps in ZnO [13]. Here, we attributed the ultrafast relaxation time (τ_f) to be excitonic thermalization via exciton–phonon scattering [14]. According to the previous time-resolved PL, the free exciton decay time is 75–100 ps in the single ZnO nanowire and 70–90 ps in ZnO bulk [11]. The obtained slow decay time (τ_s) is responsible for the radiative lifetime of free exciton.

In general, the excited free carriers will result in both the band-filling and the bandgap renormalization effects in semiconductors [17]. The band-filling (BF) or known as the Burstein–Moss effect reduces the interband transition due to the Pauli exclusion principle; the bandgap renormalization (BGR) resulting from the exchange interaction among excited carriers reduces the single-particle potential energy to cause the shrinkage of bandgap. The temporal evolution results from the interplay between BF and BGR effects can be observed in this work. For excitation energy above, the bandgap states as shown in Fig. 2(a), the BF and BGR effects emerge simultaneously by pulsed photo-excitation and compete to each other in determining the magnitude and sign of transient differential reflectance ($\Delta R/R$) at time delay of 0.67 ps. The minimal $\Delta R/R$ at time delay of 3.4 ps indicates the dominance of BGR effect. After the recovery of renormalized bandgap, the rest thermalized carriers occupy the bottom of conduction band or convert into free excitons, which the transient $\Delta R/R$ at time delay of 15 ps is attributed to the dominance of BF effect. For excitation energy corresponding to the free exciton transition as shown in Fig. 2(b), the resonantly generated carriers are ionized into free electrons via the assistance of LO-phonon to cause the screening of Coulomb interaction resulting in a reduced bandgap around zero time delay. Then the excited carriers relax to the lowest energy level via exciton–phonon scattering. After the thermalization process, the excitonic states are occupied by free excitons and the absorption saturation can be achieved by the BF effect at time delay of 4.9 ps.

3.3 Competition of band-filling and band-gap renormalization

We plotted the peak amplitude of transient normalized differential reflectance ($\Delta R/R$) at time delay of 0.67 ps as a function of excitation photon energy in Fig. 4. It reveals positive $\Delta R/R$ for 3.388 eV $< E <$ 3.444 eV and negative $\Delta R/R$ for $3.331 < E < 3.388$ eV. It is expected that the minimum of $\Delta R/R$ will occur around the bandgap energy

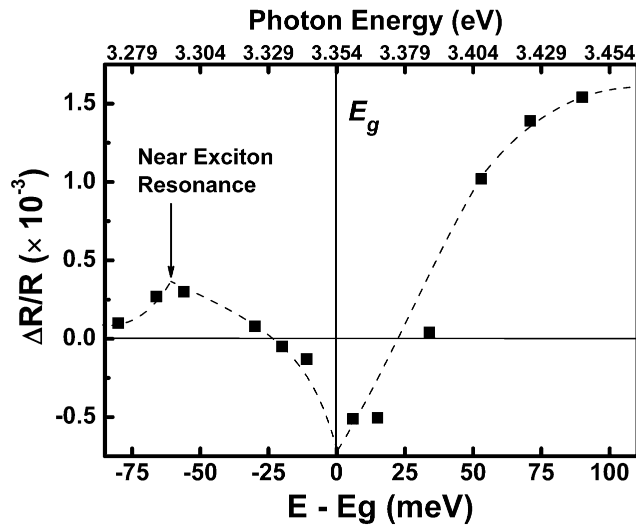

Fig. 4 The peak amplitude of measured transient differential reflectance at a time delay of 0.67 ps as a function of excitation photon energy. The *dashed lines* plotted to guide the eyes

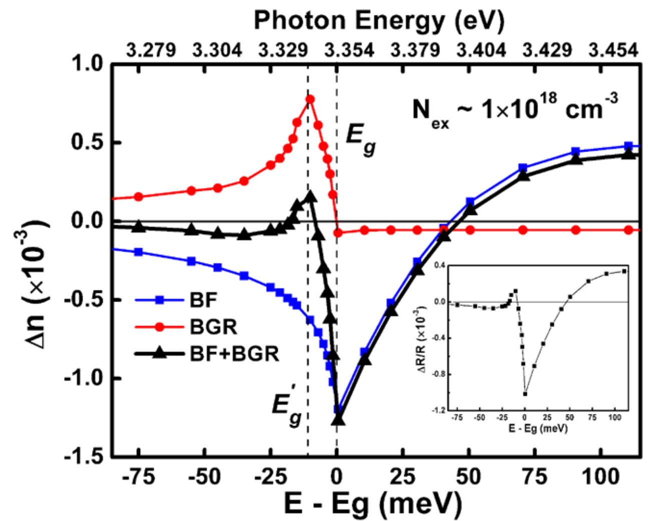

Fig. 5 Theoretical calculation of refractive index change in ZnO with spectral dependence by considering the band-filling effect (Δn_{BF}) and the bandgap renormalization effect (Δn_{BGR}) for excited carrier density of 1×10^{18} cm^{-3}. *Inset*: Theoretical calculation of normalized differential reflectance as a function of photon energy in ZnO

of 3.354 eV. The differential reflectance (ΔR) can be related to the refractive index change (Δn) resulting from redistribution of excited carriers after pulse excitation. In the case of $\Delta R/R \ll 1$, the probed normalized differential reflectance can be described as $\frac{\Delta R}{R} = \frac{4\Delta n}{n^2-1}$ [22].

According to previous literature, Bennett et al. [17] proposed a theoretical model, including the band-filling (BF) and bandgap renormalization (BGR) effects, to estimate the carrier-induced change of refractive index (Δn) in ln P under quasiequilibrium. These two effects can cause a noticeable change of refractive index especially for near bandedge states. Here, we used this model to calculate the refractive index change induced by the BF (Δn_{BF}) and BGR (Δn_{BGR}) effects in ZnO, respectively.

The absorption coefficient is assumed to obey a simple square-root law

$$\alpha_0(E) = \begin{cases} \frac{C}{E}\sqrt{E - E_g}; & E \geq E_g, \\ 0; & E < E_g, \end{cases} \tag{1}$$

where C, E, and E_g are the material constant, excitation photon energy, and the bandgap energy, respectively. The differential absorption ($\Delta\alpha$) under optical excitation is induced by the BF and BGR effects. In the case of BF effect, the spectral dependence of $\Delta\alpha_{\text{BF}}$ is given by

$$\Delta\alpha_{\text{BF}} = \alpha_0(E) \cdot (f_v - f_c - 1) \tag{2}$$

with f_v and f_c corresponding to the occupation probabilities of valence and conduction bands having the form of Fermi–Dirac distribution at RT. On the other hand, the differential absorption from BGR effect ($\Delta\alpha_{\text{BGR}}$) can be calculated by using the equation of

$$\Delta\alpha_{\text{BGR}} = \frac{C}{E}\sqrt{E - E'_g} - \alpha_0(E), \tag{3}$$

where $E'_g = E_g - \Delta E_g = E_g - \kappa \cdot \rho^{1/3}$ is the renormalized bandgap energy and ΔE_g represents the reduction of bandgap. In ZnO, κ is the coefficient of bandgap shrinkage on the order of 1.3×10^{-5} meV-cm [16], and ρ is the carrier density. By applying the Kramers–Kronig (K-K) relation to the differential absorption, the BF or BGR induced refractive index change (Δn) can be deduced to be

$$\Delta n(E) = \frac{2c\hbar}{e^2} P \int_0^\infty \frac{\Delta\alpha(E')}{E'^2 - E^2}\, dE', \tag{4}$$

where P represents for the principle value of the integral.

The excitation carrier density is estimated to be on the order of 10^{18} cm^{-3} under excitation fluence of 10 μJ/cm^2 in this work. The spectral dependences of Δn_{BF}, Δn_{BGR} and Δn for ZnO are illustrated in Fig. 5 with the carrier density of 1×10^{18} cm^{-3}. The BF produces a positive index change or $\Delta n_{\text{BF}} > 0$ with photon energy above 3.396 eV, and it decreases and transits to negative as the energy approaches E_g. The minimum of Δn_{BF} emerges at the nominal bandgap energy of 3.354 eV. On the other hand, the BGR effect with relatively small spectral dependence leads to a negative index change or $\Delta n_{\text{BGR}} < 0$ for the energy above E_g, and it leads to a positive index change for the energy below E_g. The reduction of bandgap energy (ΔE_g) is estimated to be 13 meV. It can be observed that the minimum of Δn_{BGR}

and the maximum of Δn_{BGR} are corresponding to the nominal bandgap energy and the renormalized bandgap energy, respectively. The resultant Δn due to the combined effects ($\Delta n_{\mathrm{BF}} + \Delta n_{\mathrm{BGR}}$) reveals positive for the energy well above E_g, and then becomes negative as the energy approaches E_g. The spectral dependence of calculated $\Delta R/R$ for ZnO was also shown in the inset of Fig. 5.

From the analysis above, the measurement of transient peak reflectance decreases with decreasing the photon energy for excitation above the bandgap states can be explained. As shown in Fig. 4, the competition of positive Δn_{BF} over negative Δn_{BGR} yields a positive $\Delta R/R$ for $E > 3.388$ eV. The value of $\Delta R/R$ approaches to zero for energy approaching 3.388 eV, which indicates that Δn contributed from the BF is equal to the value from the BGR effect. Due to Δn induced by the BF becomes negative or smaller than that induced by the BGR effect, it results in a negative $\Delta R/R$ for $3.331\ \mathrm{eV} < E < 3.388$ eV. The sign of transient $\Delta R/R$ gradually transits to a positive one when we further decrease the excited photon energy. Due to the contribution by near exciton resonance state ($\sim$3.294 eV), the relatively maximal $\Delta R/R$ can be observed for excitation below the bandgap energy. We noticed that the experimental result is somewhat different to the theoretical calculation especially for the photon energy below the bandgap. Due to the limitation of model, we assumed the absorption spectrum by using the square-root role for the above bandgap states without taking the excitonic state into consideration.

4 Conclusion

The spectral dependent ultrafast carrier dynamics was investigated in a ZnO epitaxial film by utilizing the femtosecond pump-probe technique at RT. Through the assistance of hot phonon emission, the free carrier thermalization time increases with the increase of photon energy. The obtained recovery time of renormalized bandgap due to the free carriers convert into free excitons is independent of photon energy. Moreover, our performance reveals the significance of competition of band-filling (BF) and bandgap renormalization (BGR) effects, which the measured transient reflectance decreases with decreasing the photon energy for excitation energy above the band-gap states. The spectral dependence of transient reflectance was confirmed by calculating the refractive index change induced by the BF and BGR effects in ZnO.

Acknowledgements This work was sponsored by the National Science Council of Taiwan under NSC 99-2221-E-009-095-MY3 and NSC 99-2112-M-027-001-MY3.

References

1. D.C. Look, Mater. Sci. Eng. B, Solid-State Mater. Adv. Technol. **80**, 383 (2001)
2. Z.K. Tang, G.K.L. Wong, P. Yu, M. Kawasaki, A. Ohtomo, H. Koinuma, Y. Segawa, Appl. Phys. Lett. **72**, 3270 (1998)
3. D.M. Bagnall, Y.F. Chen, Z. Zhu, T. Yao, S. Koyama, M.Y. Shen, T. Goto, Appl. Phys. Lett. **70**, 2230 (1997)
4. J.F. Muth, R.M. Kolbas, A.K. Sharma, S. Oktyabrsky, J. Narayan, J. Appl. Phys. **85**, 7884 (1999)
5. D.M. Bagnall, Y.F. Chen, Z. Zhu, T. Yao, M.Y. Shen, T. Goto, Appl. Phys. Lett. **73**, 1038 (1998)
6. J.H. Lin, Y.J. Chen, H.Y. Lin, W.F. Hsieh, J. Appl. Phys. **84**, 3912 (2005)
7. Y.P. Chan, J.H. Lin, C.C. Hsu, W.F. Hsieh, Opt. Express **16**, 19900 (2008)
8. J. Takeda, H. Jinnouchi, S. Kurita, Y.F. Chen, T. Yao, Phys. Status Solidi (b) **229**, 877 (2002)
9. J. Takeda, N. Arai, Y. Toshine, H.J. Ko, T. Yao, Jpn. J. Appl. Phys. **45**, 6961 (2006)
10. K.M. Kwok, A.B. Djurisic, Y.H. Leung, W.K. Chan, D.L. Phillips, Appl. Phys. Lett. **87**, 223111 (2005)
11. J.C. Johnson, K.P. Knutsen, H. Yan, M. Law, Y. Zhang, P. Yang, R.J. Saykally, Nano Lett. **4**, 197 (2004)
12. C. Bauer, G. Boschloo, E. Mukhtar, A. Hagfeldt, Chem. Phys. Lett. **387**, 176 (2004)
13. S. Acharya, S. Chouthe, C. Sturm, H. Graener, R. Schmidt-Grund, M. Grundmann, G. Seifert, J. Phys. Conf. Ser. **210**, 012048 (2010)
14. P.C. Ou, W.R. Liu, H.J. Ton, J.H. Lin, W.F. Hsieh, J. Appl. Phys. **109**, 013102 (2011)
15. P.C. Ou, J.H. Lin, C.A. Chang, W.R. Liu, W.F. Hsieh, J. Phys. D **43**, 495103 (2010)
16. J.D. Ye, S.L. Gu, S.M. Zhu, S.M. Liu, Y.D. Zheng, R. Zhang, Y. Shi, Appl. Phys. Lett. **86**, 192111 (2005)
17. B.R. Bennett, R.A. Soref, J.A. Del Alamo, IEEE J. Quantum Electron. **26**, 113 (1990)
18. W.R. Liu, W.F. Hsieh, C.H. Hsu, K.S. Liang, F.S.S. Chien, J. Cryst. Growth **297**, 294 (2006)
19. B. Guo, Z.R. Qiu, J.Y. Lin, H.X. Jiang, K.S. Wong, Appl. Phys. B **80**, 521 (2005)
20. W.Z. Lin, J.G. Fujimoto, E.P. Ippen, R.A. Logan, Appl. Phys. Lett. **50**, 124 (1987)
21. W.Z. Lin, J.G. Fujimoto, E.P. Ippen, R.A. Logan, Appl. Phys. Lett. **51**, 161 (1987)
22. A.J. Sabbah, D.M. Riffe, Phys. Rev. B **66**, 165217 (2002)